# Redox Switchable Daisy Chain Rotaxanes Driven by Radical–Radical Interactions

**ARTICLE** *in* JOURNAL OF THE AMERICAN CHEMICAL SOCIETY · FEBRUARY 2014

Impact Factor: 12.11 · DOI: 10.1021/ja500675y · Source: PubMed



**8 AUTHORS**, INCLUDING:

Carson J. Bruns
Northwestern University
**25** PUBLICATIONS **769** CITATIONS
SEE PROFILE

Marco Frasconi
University of Padova
**69** PUBLICATIONS **1,176** CITATIONS
SEE PROFILE

Severin Schneebeli
University of Vermont
**3** PUBLICATIONS **30** CITATIONS
SEE PROFILE

Chuyang Cheng
Northwestern University
**22** PUBLICATIONS **198** CITATIONS
SEE PROFILE

JACS
JOURNAL OF THE AMERICAN CHEMICAL SOCIETY
Article
pubs.acs.org/JACS

# Redox Switchable Daisy Chain Rotaxanes Driven by Radical–Radical Interactions

Carson J. Bruns,[†] Marco Frasconi,[†] Julien Iehl,[†] Karel J. Hartlieb,[†] Severin T. Schneebeli,[†] Chuyang Cheng,[†] Samuel I. Stupp,*[,†,‡,§] and J. Fraser Stoddart*[,†]

[†]Department of Chemistry [‡]Department of Materials Science and Engineering [§]Department of Medicine Northwestern University, 2145 Sheridan Road, Evanston, Illinois 60208, United States

Supporting Information

**ABSTRACT:** We report the one-pot synthesis and electrochemical switching mechanism of a family of electrochemically bistable 'daisy chain' rotaxane switches based on a derivative of the so-called 'blue box' ($BB^{4+}$) tetracationic cyclophane cyclobis(paraquat-*p*-phenylene). These mechanically interlocked molecules are prepared by stoppering kinetically the solution-state assemblies of a self-complementary monomer comprising a $BB^{4+}$ ring appended with viologen ($V^{2+}$) and 1,5-dioxynaphthalene (DNP) recognition units using click chemistry. Six daisy chains are isolated from a single reaction: two monomers (which are not formally 'chains'), two dimers, and two trimers, each pair of which contains a cyclic and an acyclic isomer. The products have been characterized in detail by high-field $^1$H NMR spectroscopy in $CD_3CN$—made possible in large part by the high symmetry of the novel $BB^{4+}$ functionality—and the energies associated with certain aspects of their dynamics in solution are quantified. Cyclic voltammetry and spectroelectrochemistry have been used to elucidate the electrochemical switching mechanism of the major cyclic daisy chain products, which relies on spin-pairing interactions between $V^{\bullet+}$ and $BB^{2(\bullet+)}$ radical cations under reductive conditions. These daisy chains are of particular interest as electrochemically addressable molecular switches because, in contrast with more conventional bistable catenanes and rotaxanes, the mechanical movement of the ring between recognition units is accompanied by significant changes in molecular dimensions. Whereas the self-complexed cyclic monomer—known as a [*c*1]daisy chain or molecular 'ouroboros'—conveys sphincter-like constriction and dilation of its ultramacrocyclic cavity, the cyclic dimer ([*c*2]daisy chain) expresses muscle-like contraction and expansion along its molecular length.

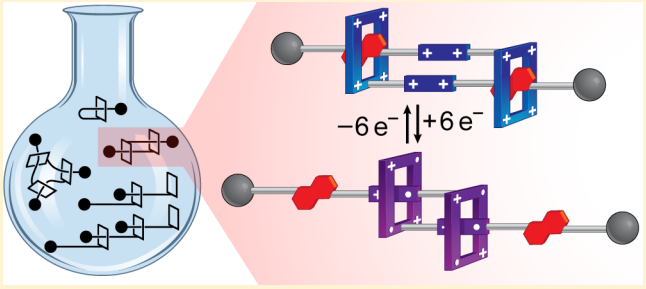


## INTRODUCTION

The continual emergence of increasingly more sophisticated and specialized molecular switches and machines is part and parcel of healthy growth and development in the field of molecular nanotechnology. Mechanically interlocked molecules[1] (MIMs) such as catenanes and rotaxanes have a prominent standing in this field because they can be designed rationally with components that express controlled mechanical motion with respect to one another to render molecular switches.[2] In bistable mechanically interlocked molecular switches, the specific topological and topographical architectures of the mechanical linkages dictate the nature of the resulting mechanical motion. Whereas the rings of a typical [2]catenane will only express rotary motion, the ring of a typical [2]rotaxane can be either circumrotated or linearly translated, and even more sophisticated motions[3] can be programmed by accessing more intricate architectures. In a world dominated by the random and erratic movements known as Brownian motion, the extent of positional discrimination between the different mechanical geometries is an important consideration because MIMs typically exist in a distribution of co-conformations. The evolution of mechanically interlocked molecular switches is thus associated both with elaborating more novel and diverse modes of motion[3] as well as higher degrees of switching fidelity. Here, we report a family of electrochemically addressable, mechanically interlocked molecular switches that constitute a step forward on both of these fronts.

Molecular 'daisy chains'[4] are a class of rotaxanes—molecules that comprise a ring encircling a rod with end groups (stoppers) that are too bulky for the ring to bypass—in which the ring and rod are directly connected by covalent bonds to form a self-complementary monomer. They are so-named because the assembly of these ring–rod monomers into cyclic or acyclic oligomers and polymers is reminiscent of the daisy chain garlands which children construct from flowers. We describe daisy chains with [*n*] components as being either acyclic [*an*] or cyclic [*cn*] assemblies. Whereas *supramolecular* daisy chains[4a,5]—the pseudorotaxane (unstoppered) analogues of molecular daisy chains—have condition-sensitive (i.e., concentration, temperature, solvent) stabilities and molecular

**Received:** January 21, 2014
**Published:** February 10, 2014



dx.doi.org/10.1021/ja500675y | *J. Am. Chem. Soc.* 2014, 136, 4714–4723

weights, the physical linkage of the mechanical bond imparts *molecular* daisy chains with the advantage of kinetic stability. Although supramolecular daisy chains can form polymeric [*an*] and [*cn*] assemblies[5a,b,e,f,h,j,6] ($n > 2$) at high concentrations, examples[7] of molecular [*an*]daisy chain polymers are rare. Instead, molecular daisy chains are typically isolated as discrete cyclic dimers,[8] with one case[9] of a cyclic trimer.

Daisy chains are of particular interest in the context of molecular switches because their actuation is accompanied by significant changes in their molecular dimensions on account of their unique cross-threaded architectures. Bistable [*c*2]daisy chains, for example, undergo a net compression or extension in molecular length as they are switched between states, for which they have earned the title of 'molecular muscles'.[10] Although the first switchable daisy chain was a chemically actuated cyclic dimer based on Sauvage's transition metal complexes,[10] the majority of daisy chain 'molecular muscles' have been photoswitchable[11] [*c*2]daisy chains based on cyclodextrin and pH-switchable[12] daisy chains based on crown ethers. A number of the pH-switchable [*c*2]daisy chains have been postfunctionalized to create larger macrocyclic[13] and polymeric[14] architectures, motivated by a growing interest[2i,14d,15] in creating materials that can scale the integrated mechanical motion of molecular machines to a macroscopic regime where they can perform work. Despite their promise as nanomechanical actuators, the variety of supramolecular motifs and corresponding stimuli for actuating daisy chains remains limited, with only one example of an electrochemically switchable donor–acceptor daisy chain.[8f]

Over the past quarter-century we have focused on the chemistry of complexes and MIMs associated with the redox-active tetracationic cyclophane cyclobis(paraquat-*p*-phenylene), known also as the little 'blue box'.[16] Blue box ($BB^{4+}$), its larger relatives,[17] and their corresponding donor–acceptor complexes and MIMs express a range of remarkable properties in the context of molecular recognition and (mechano)-stereochemistry.[18] In the ground state, $BB^{4+}$ can host a wide variety of $\pi$-electron rich aromatic guests such as 1,5-dioxynaphthalene (DNP) and redox-active tetrathiafulvalene (TTF) derivatives, which has facilitated the development of a large family molecular switches with highly tunable thermodynamic[19] and kinetic[20] properties that make them promising components for molecular electronics.[21] After two decades of donor–acceptor chemistry, our recent discovery[22] that the $BB^{2(+\bullet)}$ diradical dication forms a stable pseudorotaxane complex with viologen radical cations ($V^{+\bullet}$) via radical pairing interactions has opened up a playing field for the radical chemistry of blue box, which is proving no less remarkable as a platform for novel host–guest complexes,[23] MIMs,[24] and switches.[22,25] Here, we report a donor–acceptor templated one-pot synthesis of a family of electrochemically bistable blue box daisy chains and their radical-mediated switching properties in solution. This new class of daisy chains will be of interest for molecular nanotechnology applications that demand electrochemically addressable large-amplitude mechanical actuators on the nanoscale.

## RESULTS AND DISCUSSION

**Synthesis and Characterization of Blue Box Daisy Chains.** The nature of the connection between the ring and rod that comprise the self-complementary monomer is an important consideration for the synthesis and characterization of molecular daisy chains. If multicomponent assemblies are desired, the linker between the ring and the recognition unit should typically be short and/or rigid enough to prohibit formation of the (entropically favorable) self-complexing 'ouroboros'[26] [*c*1]daisy chain. Symmetry must also be considered because any monomer with less than a $C_2$ axis will give rise to daisy chain assemblies that express multiple stereoisomers, the number of which scales exponentially with the number of components in the assembly. In the most ubiquitous family of [*c*2]daisy chains[12−14] based on the recognition motif[27] between dibenzo[24]crown-8 and dialkylammonium ions, for example, the symmetry of the monomer is broken by the attachment of an alkylammonium moiety to one of the aromatic rings of the crown ether. These [*c*2]daisy chains therefore exist as a mixture that contains two enantiomers and a corresponding diastereoisomer.[14b] Similarly, the direct attachment of functional groups by a single covalent bond to one of the phenylene rings of blue box destroys its symmetry, giving rise to different isomers in the corresponding MIMs and inclusion complexes.[28] Although such stereochemical mixtures may not interfere with many of the intended applications of a switch or machine, the added complexity of these systems encumbers the interpretation of NMR spectra. These issues can be circumvented (Scheme 1) in blue box systems by replacing one of its phenylene (Ph) rings with a constitutionally

**Scheme 1. Synthesis of Symmetrical Azide Blue Box $BBN_3^{4+}$ and Its Transformation to the Blue Box–Viologen ($BBV^{6+}$) and Azide-Bearing Blue Box–Viologen–Naphthalene ($BBVNPN_3^{6+}$) Self-Complementary Monomers Using Click Chemistry**

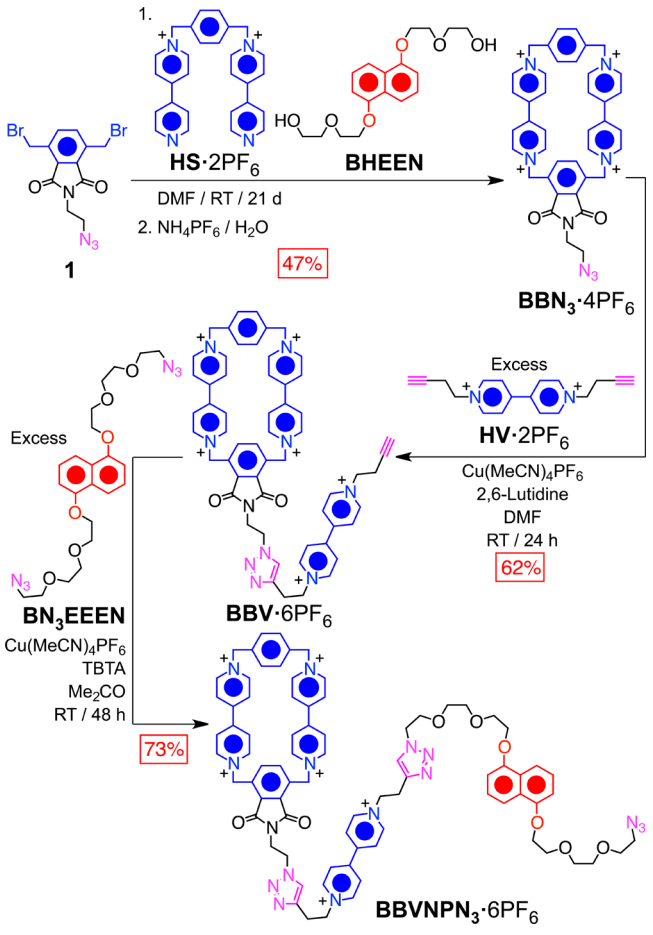



dx.doi.org/10.1021/ja500675y | J. Am. Chem. Soc. 2014, 136, 4714−4723

symmetrical phthalimide (Phth) group, such that no reduction in symmetry results from functionalizing Phth at the N position. We have used this symmetrical functionality to construct blue box supramolecular[29] and molecular[30] self-complexing (ouroboros) switches, pretzelanes,[31] and, most recently, a functionally rigid supramolecular [*c*2]daisy chain.[32]

Although a highly rigid and symmetrical linker between blue box and its recognition unit to prevent self-complexation is highly desirable, this feature comes at the cost of low yields and stabilities.[32] Instead, we reasoned that a flexible self-complementary monomer should still equilibrate between various [*a*n]- and [*c*n]daisy chain oligomers at sufficiently high concentrations, and that they could be isolated (Scheme 2) by stoppering them under kinetic control. The copper-mediated azide–alkyne 1,3-dipolar cycloaddition (CuAAC) click reaction has proven to be a remarkably useful way to form kinetically stable mechanical bonds.[33] Recently, we demonstrated[34] that multiple structurally related blue box oligorotaxanes can be isolated from a single one-pot click reaction by trapping kinetically the distribution of various supramolecular precursors at equilibrium. Analogously, we synthesized the azide-bearing blue box–viologen–naphthalene monomer **BBVNPN$_3$**$^{6+}$ with the expectation that, by using click chemistry

**Scheme 2. Click Synthesis of a Family of Monomeric, Dimeric, and Trimeric Blue Box Molecular Daisy Chains by Stoppering an Equilibrium Mixture of BBVNPN$_3$**$^{6+}$ **Assemblies**

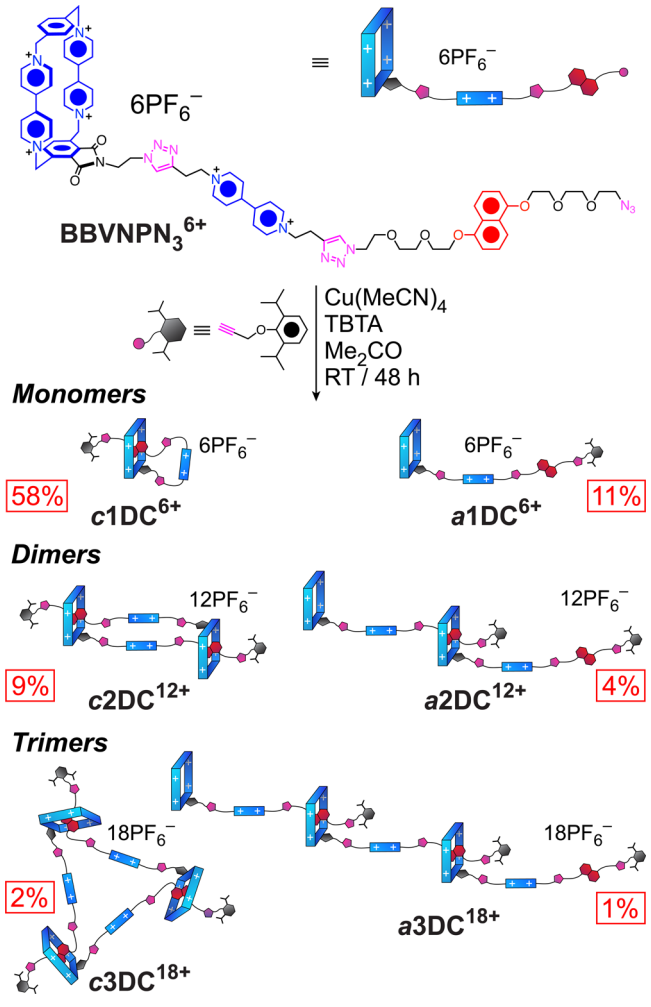


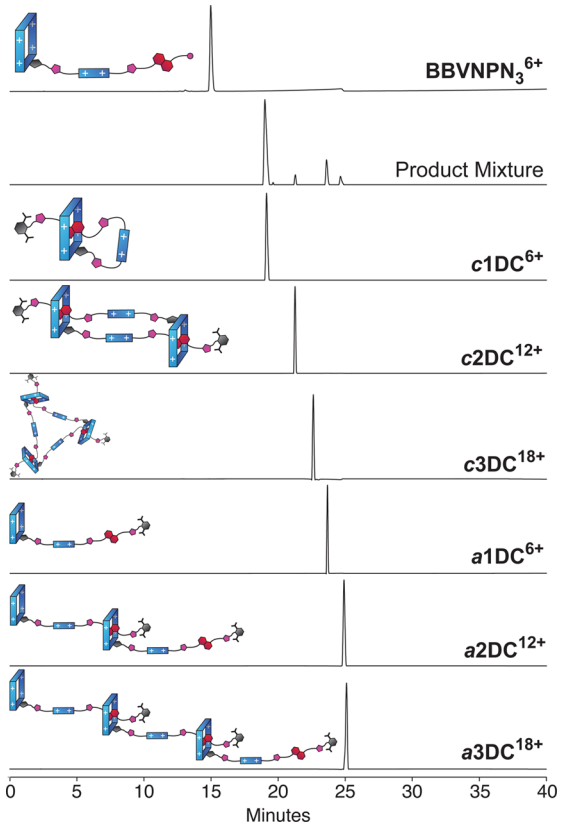


**Figure 1.** Analytical RP-HPLC chromatograms ($H_2O$–MeCN, 0.1% TFA, 0–60% MeCN in 40 min, $\lambda$ = 254 nm) of **BBVNPN$_3$**$^{6+}$, the crude product mixture from the corresponding stoppering reaction, and the isolated molecular daisy chains ***a*1DC**$^{6+}$, ***c*1DC**$^{6+}$, ***a*2DC**$^{12+}$, ***c*2DC**$^{12+}$, ***a*3DC**$^{18+}$, and ***c*3DC**$^{18+}$.

at sufficiently high concentrations, we could trap the various daisy chains in equilibrium kinetically. **BBVNPN$_3$**$^{6+}$ was synthesized (Scheme 1) via a series of click reactions from the symmetrical azide-bearing blue box precursor **BBN$_3$**$^{4+}$, which was obtained in relatively good yield from the novel Phth precursor **1**. See the Supporting Information (SI) for detailed synthetic procedures and characterization. The reaction of **BBN$_3$**$^{4+}$ with an excess of homopropargyl viologen (**HV**$^{2+}$) affords the blue box viologen monomer **BBV**$^{6+}$, which is coupled with DNP diazide **BN$_3$EEEN** in excess to afford **BBVNPN$_3$**$^{6+}$ in fair to middling yields.

We stoppered (Scheme 2) the **BBVNPN$_3$**$^{6+}$ daisy chain assemblies at a concentration of ~7 mM in $Me_2CO$ at room temperature over two days, using 40 mol % $Cu(MeCN)_4PF_6$ and TBTA ligand to catalyze the CuAAC reaction. From this one-pot synthesis we isolated the cyclic and acyclic (respectively) pairs of monomers ***c*1DC**$^{6+}$ (58%) and ***a*1DC**$^{6+}$ (11%), dimers ***c*2DC**$^{12+}$ (9%) and ***a*2DC**$^{12+}$ (4%), and trimers ***c*3DC**$^{18+}$ (2%) and ***a*3DC**$^{18+}$ (1%), for a total of six compounds in 85% yield. These compounds were separated in a routine manner by preparative-scale HPLC, eluting with $H_2O$/MeCN (0.1% TFA) in a gradient of 0–65% MeCN over 45 min. Analytical HPLC traces of the purified compounds are compared with those of the **BBVNPN$_3$**$^{6+}$ starting material and the crude product mixture in Figure 1. The chromatogram of the crude product mixture reveals the outcome of an efficient click reaction since it shows no trace of starting material, with the ***c*1DC**$^{6+}$ ouroboros as the dominant product at this


dx.doi.org/10.1021/ja500675y | *J. Am. Chem. Soc.* 2014, 136, 4714–4723

**Table 1. Formulas, Molecular Weights, and Observed Signals in the Mass Spectra of Daisy Chains *c*1DC·6PF$_6$, *a*1DC·6PF$_6$, *c*2DC·12PF$_6$, *a*2DC·12PF$_6$, *c*3DC·18PF$_6$, and *a*3DC·18PF$_6$**

| | | MW | HRMS signals (*m*/*z*) | | |
|---|---|---|---|---|---|
| cmpd | formula | (g·mol$^{-1}$) | ion | calculated | observed |
| ***c*1DC**·6PF$_6$ | $C_{95}H_{102}F_{36}N_{16}O_9P_6$ | 2481.713 | $[M - PF_6]^+$ | 2336.6253 | 2336.6131 |
| | | | $[M - 2PF_6]^{2+}$ | 1095.8303 | 1095.8306 |
| | | | $[M - 3PF_6]^{3+}$ | 682.2320 | 682.2358 |
| ***a*1DC**·6PF$_6$ | $C_{95}H_{102}F_{36}N_{16}O_9P_6$ | 2481.713 | $[M - PF_6]^+$ | 2336.6253 | 2336.6552 |
| | | | $[M - 2PF_6]^{2+}$ | 1095.8303 | 1095.8322 |
| | | | $[M - 3PF_6]^{3+}$ | 682.2320 | 682.2357 |
| ***c*2DC**·12PF$_6$ | $C_{190}H_{204}F_{72}N_{32}O_{18}P_{12}$ | 4963.427 | $[M - 2PF_6]^{2+}$ | 2336.6253 | 2336.6274 |
| | | | $[M - 3PF_6]^{3+}$ | 1509.4286 | 1509.4334 |
| | | | $[M - 4PF_6]^{4+}$ | 1095.8303 | 1095.8298 |
| ***a*2DC**·12PF$_6$ | $C_{190}H_{204}F_{72}N_{32}O_{18}P_{12}$ | 4963.427 | $[M - 2PF_6]^{2+}$ | 2336.6253 | 2336.6435 |
| | | | $[M - 3PF_6]^{3+}$ | 1509.4286 | 1509.4279 |
| | | | $[M - 4PF_6]^{4+}$ | 1095.8303 | 1095.8301 |
| | | | $[M - 5PF_6]^{5+}$ | 847.6713 | 847.6773 |
| ***c*3DC**·18PF$_6$ | $C_{285}H_{306}F_{108}N_{48}O_{27}P_{18}$ | 7445.140 | $[M - 3PF_6]^{3+}$ | 2336.6253 | 2336.6349 |
| | | | $[M - 4PF_6]^{4+}$ | 1716.2278 | 1716.2111 |
| | | | $[M - 5PF_6]^{5+}$ | 1343.9893 | 1343.9868 |
| ***a*3DC**·18PF$_6$ | $C_{285}H_{306}F_{108}N_{48}O_{27}P_{18}$ | 7445.140 | $[M - 3PF_6]^{3+}$ | 2336.6253 | 2336.6262 |
| | | | $[M - 4PF_6]^{4+}$ | 1716.2278 | 1716.2740 |
| | | | $[M - 5PF_6]^{5+}$ | 1343.9893 | 1343.9834 |

concentration. Although optimizing the reaction to favor a particular product was outside the scope of this work, we expect that raising the concentration would bias the product distribution further toward dimers, trimers, and larger oligomers.

The blue box daisy chains were characterized by high-resolution mass spectrometry (HRMS). Since all of the compounds are constituted by identical monomers, they all produce signals at $m/z$ = 2336, corresponding to $[M - PF_6]^+$, $[M - 2PF_6]^{2+}$, and $[M - 3PF_6]^{3+}$ for the monomers, dimers, and trimers, respectively, with isotope patterns that characterize singly, doubly, and triply charged ions. We also observed signals for the dimers and trimers that are not expressed by monomers, for example $[M - 3PF_6]^{3+}$ at $m/z$ = 1509 for the dimers and $[M - 4PF_6]^{4+}$ at $m/z$ = 1716 for the trimers. These observed signals are compared with the calculated mass spectra in Figure S1 of the SI, and tabulated in Table 1.

The monomers and dimers were isolated in sufficient quantities for detailed spectroscopic and electrochemical characterization. The charge-transfer interactions between the DNP unit and the tetracationic cyclophane were monitored using visible absorption spectroscopy. The extinction coefficients of ***a*1DC$^{6+}$**, ***c*1DC$^{6+}$**, ***a*2DC$^{12+}$**, and ***c*2DC$^{12+}$** in MeCN are compared in Figure 2. The three daisy chains that host a DNP unit within BB$^{4+}$ (***c*1DC$^{6+}$**, ***a*2DC$^{12+}$**, and ***c*2DC$^{12+}$**) all express a visible absorption band with a $\lambda_{max}$ of approximately 530 nm, attributable to the charge transfer absorption between BIPY$^{2+}$ and DNP in the DNP⊂BB$^{4+}$ 'subcomplex'.[35] On the contrary, the uncomplexed ***a*1DC$^{6+}$** monomer has a comparatively weaker absorption at $\lambda_{max}$ = 475 nm, corresponding to a weaker side-on DNP−V$^{2+}$ interaction, most likely between the two recognition units in the dumbbell component appended to BB$^{4+}$. The extinction coefficient of the charge transfer band at 530 nm scales with the number of DNP⊂BB$^{4+}$ subcomplexes in the daisy chain, providing an explanation why the doubly complexed ***c*2DC$^{12+}$** molecule has a higher extinction coefficient than its ***c*1DC$^{6+}$** and ***a*2DC$^{12+}$** homologues. The daisy chains can also be distinguished (section 4 of the SI) by $^1$H NMR spectroscopy.

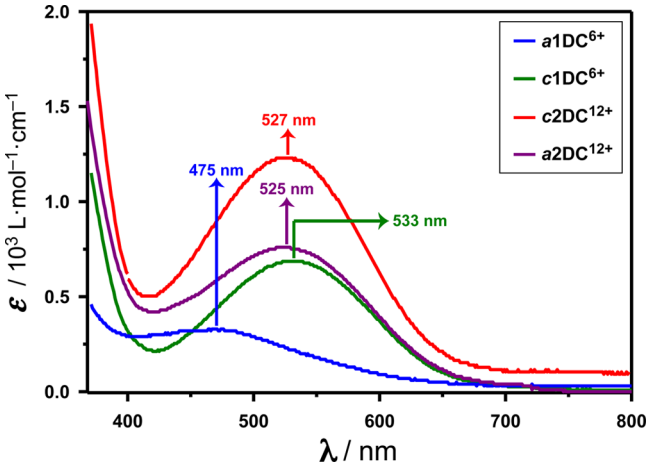


**Figure 2.** Extinction coefficients of the charge transfer absorption bands of ***a*1DC$^{6+}$**, ***c*1DC$^{6+}$**, ***c*2DC$^{12+}$**, and ***a*2DC$^{12+}$**.

**Isomerism and Dynamics of Blue Box Daisy Chains.** We used $^1$H NMR spectroscopy to investigate the isomerism and dynamics of the daisy chains in $CD_3CN$. The daisy chains are most easily understood with reference to the simplest monomeric compounds; the $^1$H NMR spectra of ***a*1DC$^{6+}$** and ***c*1DC$^{6+}$** are compared at 298 K in Figure 3. The spectrum of the uncomplexed monomer ***a*1DC$^{6+}$** is particularly simple because it does not host a DNP⊂BB$^{4+}$ subcomplex within its structure. ***a*1DC$^{6+}$** has time-averaged $C_{2v}$ symmetry, with two sets of BB$^{4+}$ signals for the $\alpha$, $\beta$, and methylene units. Each of these signals is doubled in ***c*1DC$^{6+}$** because the local constitutional asymmetry of the DNP unit is imposed on the cyclophane while hindering the free rotation of its aromatic rings. In addition to this differentiation of the BB$^{4+}$ signals, the protons associated with BB$^{4+}$ and DNP in ***c*1DC$^{6+}$** are dramatically shifted with respect to those of ***a*1DC$^{6+}$**. The protons at the 4/8 positions of DNP undergo a particularly


dx.doi.org/10.1021/ja500675y | J. Am. Chem. Soc. 2014, 136, 4714−4723

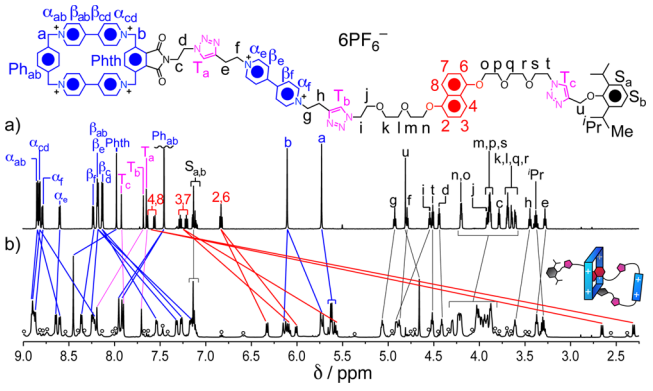


**Figure 3.** Comparison of the $^1$H NMR spectra ($CD_3CN$, 600 MHz, 298 K) of (a) ***a*1DC$^{6+}$** and (b) ***c*1DC$^{6+}$**.

large shift (~5 ppm) to lower frequencies because they are directed into the shielding cone of the phenylene (Ph) and phthalimide (Phth) units of BB$^{4+}$ by [C−H···$\pi$] interactions. The $^1$H NMR spectrum of ***c*1DC$^{6+}$** also shows a second set of small signals—annotated with open circles in Figure 3—that represent a minor co-conformation, which equilibrates slowly with the major co-conformation on the $^1$H NMR time scale. On the basis of signal integration, this minor co-conformational isomer of ***c*1DC$^{6+}$** represents approximately 15% of the molecular population.

The isomerism of the daisy chains can be rationalized by considering the dynamic processes associated with the DNP⊂BB$^{4+}$ subcomplex shown in Scheme 3. In Process I, the DNP unit pirouettes about its central C−C bond to transpose the positions of its protons at the 4/8 positions with respect to the Ph and Phth rings. To aid the discussion we will refer to co-conformations in which $H_8$ is directed toward Phth as '*DNP-Up*', while '*DNP-Down*' will represent isomers in which $H_4$ points toward Phth. In Process II, the Phth ring rotates 180° around the axis that passes through the methylene groups to reverse the direction of the imide unit. '*Phth-Out*' denotes isomers in which the imide unit is directed toward the stopper ($R^3$ in Scheme 3), while '*Phth-In*' signifies isomers in which Phth points away from the stopper. The combination of these two binary processes renders up to four co-conformational isomers for this type of DNP⊂BB$^{4+}$ subcomplex.[36] Thus, the 4/8 DNP and Phth proton signals serve as probes for evaluating the distribution of isomers and activation energies associated with Processes I and II. Four Phth signals and eight 4/8-DNP signals can be expected in the $^1$H NMR spectrum of a daisy chain if all four co-conformations illustrated in Scheme 3 are populated. The fact that ***c*1DC$^{6+}$** has only half of the expected number of signals—corresponding to only two isomers—suggests that one of these processes is forbidden (vide infra) in this molecule. In contrast with ***c*1DC$^{6+}$**, all four possible co-conformations of the DNP⊂BB$^{4+}$ subcomplex are populated in the cyclic dimer ***c*2DC$^{12+}$**, giving rise to a more complicated $^1$H NMR spectrum. Again one isomer is dominant, representing almost two-thirds of the distribution, which was found to be 7:14:15:64 by signal integration. Although the protons of minor isomers were not assigned to their corresponding signals, the major isomers of ***c*1DC$^{6+}$** and ***c*2DC$^{12+}$** have both been ascribed (sections 4.2 and 4.3 of the SI) to the *DNP-Up*/*Phth-In* co-conformations as a result of 2D NMR spectroscopic analysis.

The partial VT $^1$H NMR spectra of ***c*1DC$^{6+}$** and ***c*2DC$^{12+}$** showing the Phth and 4/8-DNP probe signals are compared over the range of −10 to 80 °C in Figure 4. The two assemblies exhibit significantly different behaviors. Whereas the four 4/8 DNP signals of ***c*1DC$^{6+}$** coalesce into a pair of signals at 60 °C,

**Scheme 3. Exchange of the Four Stable Co-Conformations Associated with Pirouetting of the DNP Unit (Process I) and Rotation of the Phth Unit (Process II)**

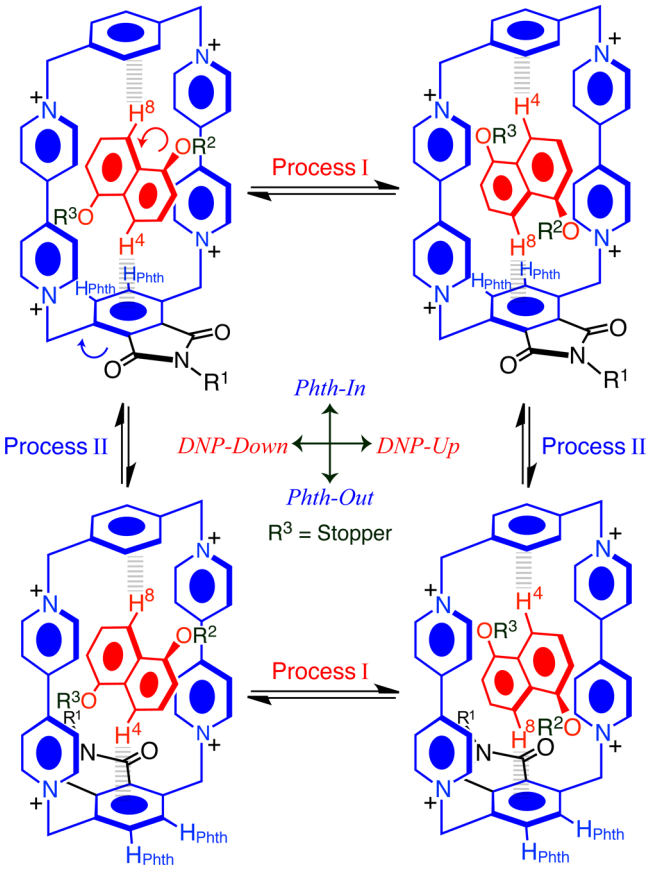


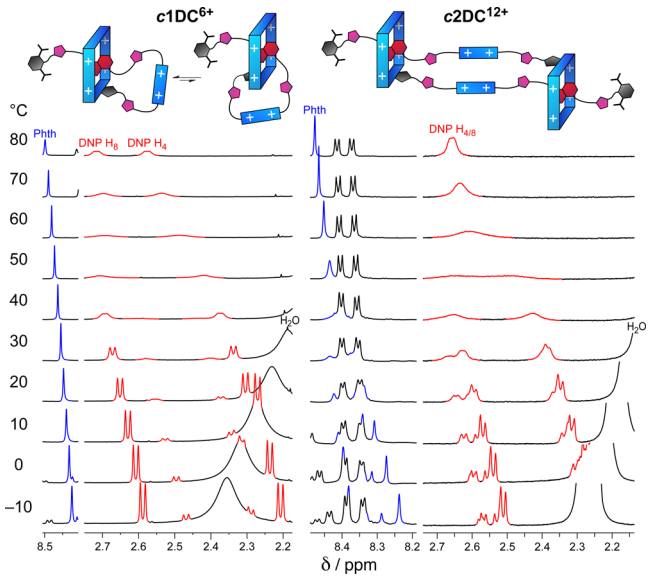


**Figure 4.** Comparison of the partial VT $^1$H NMR spectra ($CD_3CN$, 600 MHz) of ***c*1DC$^{6+}$** (left) and ***c*2DC$^{12+}$** (right) showing the Phth and 4/8 DNP signals from −10 to 80 °C.


dx.doi.org/10.1021/ja500675y | J. Am. Chem. Soc. 2014, 136, 4714−4723

Table 2. Estimations of the Rates and Energies of Exchange Processes I and II in Daisy Chains *c*1DC$^{6+}$, *c*2DC$^{12+}$, *c*3DC$^{18+}$, and *a*2DC$^{12+}$ Based on Signal Coalescence in their VT $^1$H NMR spectra

| | process I: DNP rotation | | | process II: Phth rotation | | |
|---|---|---|---|---|---|---|
| cmpd | $T_{cI}$ (°C) | $k_{cI}$ ($s^{-1}$)[a] | $\Delta G^{\ddagger}$(kcal·mol$^{-1}$) | $T_{cII}$ (°C) | $k_{cII}$ ($s^{-1}$)[b] | $\Delta G^{\ddagger}$ (kcal·mol$^{-1}$) |
| *c*1DC$^{6+}$ | – | – | >17 | 60 | 133 | 16.3 |
| *c*2DC$^{12+}$ | 50 | 307 | 15.3 | 40 | 93 | 15.5 |
| *c*3DC$^{18+}$ | 50 | 333 | 15.2 | 30 | 67 | 15.2 |
| *a*2DC$^{12+}$ | 40 | 318 | 14.8 | 15 | 22 | 15.0 |

[a]The rate of process I at the coalescence temperature $k_{cI}$ is based on the average peak separation between the 4 and 8 DNP protons at the coalescence temperature $T_{cII}$. [b]The rate of process II at the coalescence temperature $k_{cII}$ is based on the peak separation between the coalescing DNP proton signals at −30 °C.

the two sets of four DNP signals arising from *c*2DC$^{12+}$ coalesce simultaneously near 40 °C into a pair of broad signals, which appear to coalesce at 50 °C to give only one signal. Since the 4 and 8 DNP protons are constitutionally heterotopic, this apparently singular signal above 50 °C in *c*2DC$^{12+}$ formally comprises two overlapping resonances; their identical frequencies, however, suggest that these DNP protons sample nearly identical time-averaged chemical environments on the $^1$H NMR time scale at high temperatures. The 4/8 DNP protons of the cyclic trimer *c*3DC$^{18+}$ and acyclic dimer *a*2DC$^{12+}$ also express a double coalescence into what appears to be one signal at high temperatures. See sections 4.4 and 4.5 of the SI. On the contrary, the two 4/8 DNP signals of *c*1DC$^{6+}$ remain markedly separated even at 80 °C. These data indicate that Process I is the forbidden dynamic in *c*1DC$^{6+}$, since the 4 and 8 DNP protons should resonate at approximately the same frequency when Process I is fast on the NMR time scale. Thus, the activation barrier—as a weighted average—to Process II in *c*1DC$^{6+}$ has been estimated to be approximately 16.3 kcal·mol$^{-1}$ from the separation frequencies and coalescence temperature ($T_{cII}$ = 60 °C) of the 4/8 DNP proton signals.

Since both Processes I and II are active in daisy chains *c*2DC$^{12+}$, *c*3DC$^{18+}$, and *a*2DC$^{12+}$, their 4/8 DNP signals are characterized by two coalescence temperatures. In all of the daisy chain $^1$H NMR spectra, the 4/8 DNP proton signals are clustered into one of two regions. Through-space $^1$H−$^1$H correlations determined from nuclear Overhauser effect spectroscopy (Figures S7 and S13 in the SI) reveals that the set of DNP protons resonating at higher frequencies are directed into the Phth ring, while those that resonate at lower frequencies are directed into the Ph ring. Therefore, the coalescence of the cluster of DNP signals that resonate at higher frequencies (>2.45 ppm below room temperature) reflects the rate of Process II (in Figure 4, $T_{cII}$ = 40 °C for *c*2DC$^{12+}$). Since the merging of these two separate clusters into a single frequency represents the site exchange of DNP $H_4$ and $H_8$, we assume that this second 'coalescence' (in Figure 4, $T_{cI}$ = 50 °C for *c*2DC$^{12+}$) can be used to estimate the energy barrier for Process I. Activation barriers to Processes I and II were calculated from the separation frequencies and coalescence temperatures of four daisy chains and are listed in Table 2. Although they are provisory, these estimations reveal the trend, *c*1DC$^{6+}$>*c*2DC$^{12+}$>*c*3DC$^{18+}$>*a*2DC$^{12+}$, with respect to $\Delta G^{\ddagger}$ values for Processes I and II, an observation which is consistent with the expectation that the energy barriers associated with the dynamics of the DNP⊂BB$^{4+}$ subcomplex should decrease with increasing degrees of freedom in the daisy chains because of the lifting of steric and electrostatic constraints. An equal distribution of co-conformational isomers detected in the $^1$H NMR spectra of *c*3DC$^{18+}$ and *a*2DC$^{12+}$ (sections 4.4 and 4.5 in the SI) also suggests that the smaller ultramacrocycles constituting *c*1DC$^{6+}$ and *c*2DC$^{12+}$ constrain their dynamics and isomerism.

In summary, the different co-conformational isomers related to exchange Processes I and II in the DNP⊂BB$^{4+}$ 'subcomplex' of the daisy chains are biased toward the *DNP-Up/Phth-In* isomers in the smaller, more restricted cyclic compounds *c*1DC$^{6+}$ and *c*2DC$^{12+}$, whereas the isomers appear to exist in approximately equal ratios in the more flexible *c*3DC$^{18+}$ and *a*2DC$^{12+}$ daisy chains. The pirouetting of DNP (Process I) is forbidden only in *c*1DC$^{6+}$, which is most likely related to the relatively small size of the ultramacrocycle comprising its self-complexed structure, affording a more limited range of conformational freedom than that experienced by the larger homologues. Correspondingly, the activation energies associated with DNP and Phth rotation (Processes I and II, respectively) decrease with increasingly large (more flexible) cyclic daisy chains, and are lowest in the acyclic (most flexible) [*a*2]daisy chain.

**Electrochemical Switching of Blue Box Daisy Chains.** The interaction between blue box (BB$^{4+}$) and its appended viologen (V$^{2+}$) unit is an unfavorable one on account of electrostatic repulsion. As such, nearly all of the rings of the daisy chains encircle DNP in the ground state, reflecting an excellent positional bias between the switches' two stations. Our previous work[22−25] on the radical chemistry of blue box led us to expect that, under reductive conditions, the diradical dicationic BB$^{2(\bullet+)}$ would move to the radical cationic V$^{\bullet+}$ to support a V$^{\bullet+}$⊂BB$^{2(\bullet+)}$ interaction. This radical inclusion 'complex' can be detected by its signature features in the cyclic voltammogram (CV) and visible/near-infrared absorption profile observed using spectroelectrochemical techniques. All CV and spectroelectrochemistry was performed in Ar-purged MeCN with 0.1 M $NBu_4PF_6$ as a supporting electrolyte and referenced against a Ag/AgCl electrode.

We first characterized the redox behavior of the **BBV**$^{6+}$ monomer to verify that the V$^{\bullet+}$ radical cation becomes included within the cavity of the BB$^{2(\bullet+)}$ diradical dication on account of favorable radical−radical interactions, and determine whether the linkage between BB$^{2(\bullet+)}$ and V$^{\bullet+}$ units leads to a self-complexed ouroboros entity or multicomponent supramolecular daisy chain assemblies in the absence of a mechanical bond. The CV of **BBV**$^{6+}$ is compared with **HV**$^{2+}$ and **BBN$_3$**$^{4+}$ as control compounds at a scan rate of 100 mV·s$^{-1}$ in Figure 5. The first reduction wave of **BBV**$^{6+}$ is a three-electron process occurring at a peak potential of −326 mV, corresponding to three reductions: two electrons are transferred to BB$^{4+}$ (BB$^{4+}$→BB$^{2(\bullet+)}$) to reduce each of its bipyridinium units, and one electron is passed to the LUMO of the appended viologen unit (V$^{2+}$→V$^{\bullet+}$). This reduction is shifted positively with respect to


dx.doi.org/10.1021/ja500675y | J. Am. Chem. Soc. 2014, 136, 4714−4723

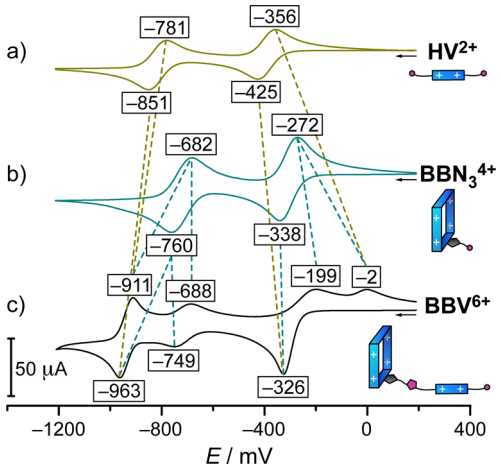


**Figure 5.** Comparison of the CV (MeCN, 0.1 M $NBu_4PF_6$, 100 mV·$s^{-1}$) of 1 mM solutions of (a) $\mathbf{HV}^{2+}$, (b) $\mathbf{BBN_3}^{4+}$, and (c) $\mathbf{BBV}^{6+}$ against Ag/AgCl.

the $\mathbf{HV}^{2+}$ and $\mathbf{BBN_3}^{4+}$ controls (−425 and −338 mV, respectively) because radical−radical interactions stabilize a trisradical $V^{\bullet+}\subset BB^{2(\bullet+)}$ subcomplex within $\mathbf{BBV}^{3(\bullet+)}$. The second reduction of the three bipyridinium radical cations ($BIPY^{\bullet+}$) of $\mathbf{BBV}^{3(\bullet+)}$ to the fully neutral **BBV** species occurs in two separate processes with peak potentials of −749 and −943 mV. The one-electron process at −749 mV is assigned to the reduction of one of the two $BIPY^{\bullet+}$ units of $BB^{2(\bullet+)}$ which is not engaged as strongly in radical pairing interactions ($BB^{2(\bullet+)}\rightarrow BB^{\bullet+}$). The final two-electron process at −963 mV corresponds to the neutralization of the spin-paired $V^{\bullet+}\subset BB^{\bullet+}$ subcomplex ($V^{\bullet+}\rightarrow V$ and $BB^{\bullet+}\rightarrow BB$), which is shifted to substantially more negative potentials than those of the $\mathbf{HV}^{\bullet+}$ and $\mathbf{BBN_3}^{2(\bullet+)}$ controls (−851 and −760 mV, respectively) because of the favorable interactions that characterize the expected radical pair inside the cyclophane of $\mathbf{BBV}^{3(\bullet+)}$. Reoxidation of the neutral **BBV** species to the $\mathbf{BBV}^{3(\bullet+)}$ trisradical is a reversible process, whereas the oxidation of $\mathbf{BBV}^{3(\bullet+)}$ back to $\mathbf{BBV}^{6+}$ occurs as a two-step process: a one-electron transfer at a peak potential of −199 mV, followed by another two-electron transfer occurring at −2 mV. We propose that steric constraints, reminiscent of ring strain, are imposed on the short linkage between the viologen and blue box units in the self-complexed co-conformation, and that they raise the energy barrier to relaxation from this state enough to stabilize the bisradical tetracationic intermediate $V^{\bullet+}\subset BB^{(2+)(\bullet+)}$. The hypothesis of the existence of the bisradical intermediate $V^{\bullet+}\subset BB^{(2+)(\bullet+)}$ is supported (Figure S20a in the SI) by variable scan rate CV experiments. The voltammograms show a growth in intensity of the final two-electron oxidation process with increasing scan rate, a phenomenon which is related to the rate of dissociation of the $V^{\bullet+}\subset BB^{(2+)(\bullet+)}$ subcomplex into uncomplexed components. The energy related to this process is consistent with our previous observations[24c] of $V^{\bullet+}\subset BB^{(4+)}$ radicals that are stabilized by sterically demanding mechanical bonds. The visible/near-IR absorption spectrum of the $\mathbf{BBV}^{3(\bullet+)}$ trisradical (Figure S20b in the SI) is characteristic of $V^{\bullet+}\subset BB^{2(\bullet+)}$ interactions (vide infra) even at very low concentrations, with an extinction coefficient which does not change over the range of 1−100 μM. See Figure S21b in the SI. We also characterized the 1:1 $\mathbf{HV}^{\bullet+}\subset\mathbf{BBN_3}^{2(\bullet+)}$ complex (section 5.1 of the SI) and showed that, in contrast with $\mathbf{BBV}^{3(\bullet+)}$, it is primarily dissociated at 20 μM. We therefore conclude that the covalent tether connecting $V^{\bullet+}$ and $BB^{2(\bullet+)}$ enables their interaction across all concentrations of $\mathbf{BBV}^{3(\bullet+)}$, meaning a [*c*1] ouroboros assembly is adopted.

The $\mathbf{HV}^{2+}$, $\mathbf{BBN_3}^{4+}$, and $\mathbf{BBV}^{6+}$ data provided a context for the electrochemical characterization of the molecular daisy chain assemblies. The CV of the uncomplexed monomer $\boldsymbol{a}\mathbf{1DC}^{6+}$ is compared with daisy chains $\boldsymbol{c}\mathbf{1DC}^{6+}$, $\boldsymbol{c}\mathbf{2DC}^{12+}$, and $\boldsymbol{a}\mathbf{2DC}^{12+}$ in Figure 6. The CV of $\boldsymbol{a}\mathbf{1DC}^{6+}$ closely resembles the superimposition of controls $\mathbf{HV}^{2+}$ and $\mathbf{BBN_3}^{4+}$, indicating that no inclusion complex is formed in this monomer under reduced conditions, according to expectations. On the contrary, the CVs of the remaining daisy chains express the features expected for $V^{\bullet+}\subset BB^{2(\bullet+)}$ interactions, with first reduction potentials that are shifted more positively and final reduction potentials that are shifted more negatively with respect to $\boldsymbol{a}\mathbf{1DC}^{6+}$ on account of spin-pairing interactions that stabilize the viologen and blue box radical cations within the daisy chains. Since $\boldsymbol{c}\mathbf{1DC}^{6+}$ possesses the same self-complexed architecture as $\mathbf{BBV}^{6+}$, their CVs are almost identical, with the same redox processes occurring at slightly different potentials. In $\boldsymbol{c}\mathbf{2DC}^{12+}$, a six-electron reduction process ($\boldsymbol{c}\mathbf{2DC}^{12+}\rightarrow\boldsymbol{c}\mathbf{2DC}^{6(\bullet+)}$) occurs at a peak potential of −326 mV to generate two trisradical $V^{\bullet+}\subset BB^{2(\bullet+)}$ subcomplexes within the molecule. A two-electron process at −741 mV corresponding to the one-electron reduction of an unpaired $BIPY^{\bullet+}$ unit of each $V^{\bullet+}\subset BB^{2(\bullet+)}$ subcomplex ($V^{\bullet+}\subset BB^{2(\bullet+)}\rightarrow V^{\bullet+}\subset BB^{\bullet+}\times 2$) gives $\boldsymbol{c}\mathbf{2DC}^{4(\bullet+)}$, which is finally neutralized to $\boldsymbol{c}\mathbf{2DC}$ at the negatively shifted potential of −1032 mV. In contrast with the [*c*1] ouroboros assemblies, these processes are reversible in the [*c*2]daisy chain, where a highly positively shifted final reoxidation wave akin to that of $\mathbf{BBV}^{6+}$ or $\boldsymbol{c}\mathbf{1DC}^{6+}$ is not observed at this scan rate. Variable scan-rate CVs (Figure S22) of these cyclic daisy chains are discussed in section 5.3 of the SI. The redox processes in $\boldsymbol{a}\mathbf{2DC}^{12+}$, which are also reversible with a significant broadening of peaks, constitute what amounts to a superimposition of $\boldsymbol{a}\mathbf{1DC}^{6+}$ and $\boldsymbol{c}\mathbf{2DC}^{12+}$, since both interlocked and noninterlocked $V^{\bullet+}$ and $BB^{2(\bullet+)}$ radicals are generated in this species.

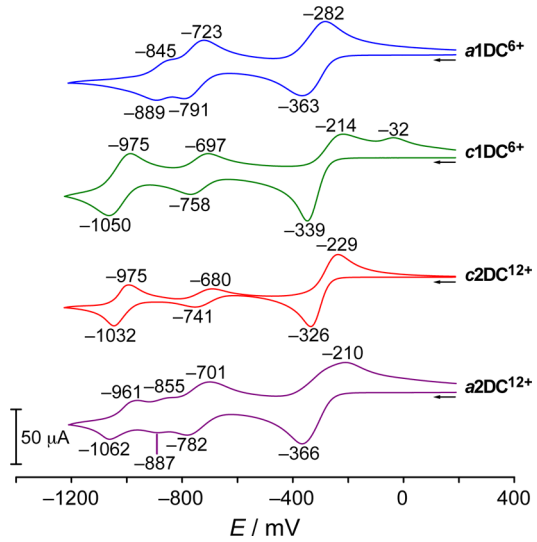


**Figure 6.** Comparison of the CV (MeCN, 0.1 M $NBu_4PF_6$, 100 mV·$s^{-1}$) of 1 mM solutions of (a) $\mathbf{a1DC}^{6+}$, (b) $\mathbf{c1DC}^{6+}$, (c) $\boldsymbol{c}\mathbf{2DC}^{12+}$, and (d) $\boldsymbol{a}\mathbf{2DC}^{12+}$ against Ag/AgCl.

The mechanism for the redox switching of the daisy chains was also examined by visible/near-IR absorption spectroscopy


dx.doi.org/10.1021/ja500675y | J. Am. Chem. Soc. 2014, 136, 4714−4723

(Figure 7) of electrochemically generated radical species. The absorption profile of ***c*2DC**$^{12+}$ throughout its redox-activated

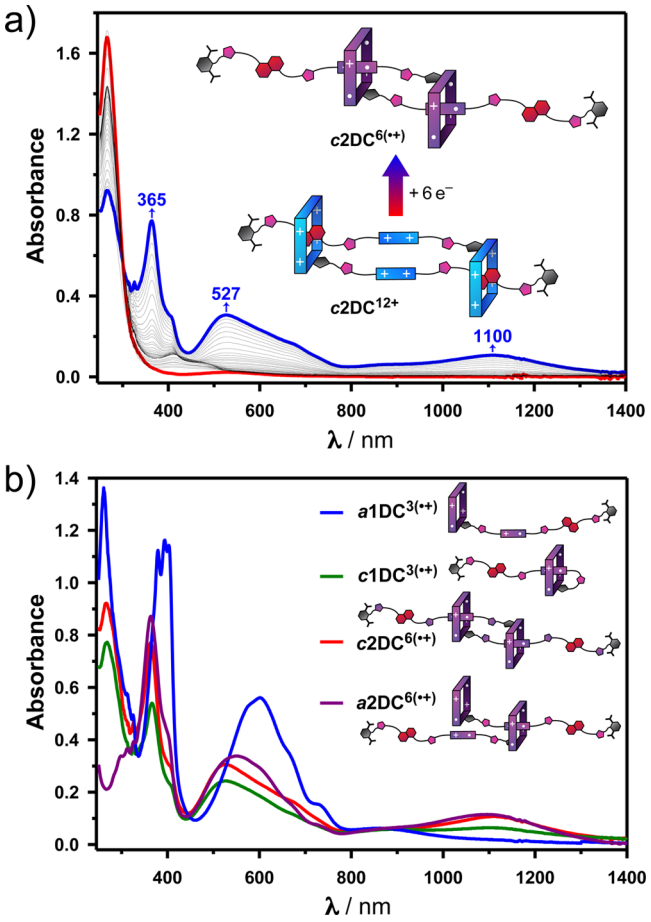


**Figure 7.** Spectroelectrochemistry of blue box daisy chains. (a) Visible/near-IR absorption profile of ***c*2DC**$^{12+}$ throughout its transition from a contracted form in the ground state (red curve) to the extended geometry of the ***c*2DC**$^{6(\bullet+)}$ radical species (blue curve) at a sustained applied voltage of −550 mV (scans taken every 2 min). (b) The visible/near-IR absorption profiles of ***a*1DC**$^{3(\bullet+)}$ (blue), ***c*1DC**$^{3(\bullet+)}$ (green), ***c*2DC**$^{6(\bullet+)}$ (red), and ***a*2DC**$^{6(\bullet+)}$ (violet) at an applied voltage of −550 mV. All of the compounds except for the noninterlocked ***a*1DC**$^{3(\bullet+)}$ monomer have broad absoprtion bands centered near 1100 nm that characterize the $V^{\bullet+}\subset BB^{2(\bullet+)}$ interaction.

transition to ***c*2DC**$^{6(\bullet+)}$ is shown as a representative example in Figure 7a. The appearance and gradual growth of new absorption bands at 365 and 527 nm, typical of viologen radical-cation species, is observed at an applied reducing voltage of −0.55 V. Importantly, the appearance of a new set of peaks, centered at approximately 890 and 1110 nm, are also observed. These absorption bands are characteristic of 'pimerized' $V^{\bullet+}$ radicals,[37] verifying that the $BB^{2(\bullet+)}$ rings of the daisy chain move to encircle the $V^{\bullet+}$ radical cations under reducing conditions. The absorption spectra of all four of the reduced monomeric and dimeric compounds are compared at −0.55 V in MeCN in Figure 7b. Like ***c*2DC**$^{6(\bullet+)}$, the ***c*1DC**$^{3(\bullet+)}$ absorption bands are characteristic of the spin-paired radicals of the expected $V^{\bullet+}\subset BB^{2(\bullet+)}$ subcomplex. On the contrary, the monomer ***a*1DC**$^{3(\bullet+)}$ trisradical species lacks the broad absorption band centered near 1100 nm that characterizes the pimers of the $V^{\bullet+}\subset BB^{2(\bullet+)}$ subcomplex, and the visible absorption bands at 380 and 600 nm are red-shifted relative to the other daisy chains. This absorption profile more closely resembles a superimposed spectrum (Figure S19b in the SI) of **HV**$^{\bullet+}$ and **BBN**$_3^{2(\bullet+)}$ and is mostly consistent with that of unpaired $V^{\bullet+}$ radical cations, confirming that no inclusion complex is formed in ***a*1DC**$^{3(\bullet+)}$. A small broad absorption centered at 860 nm, however, is indicative of a weak side-on spin-pairing interaction between $V^{\bullet+}$ and one of the $BIPY^{\bullet+}$ radical cations of $BB^{2(\bullet+)}$. Finally, the spectrum of the ***a*2DC**$^{6(\bullet+)}$ dimer was found once again to resemble a superimposed spectrum of ***a*1DC**$^{3(\bullet+)}$ and the [*cn*]daisy chains, with a broader range of absorption bands on account of the presence of pimerized radical-cation species from both interlocked and noninterlocked $V^{\bullet+}$ and $BB^{2(\bullet+)}$ segments. The absorption spectra of each of these reduced daisy chains are compared with their counterparts in the ground state in Figure S23 of the SI.

The changes in dimension of the daisy chains which accompany their mechanical switching is noteworthy for potential applications of molecular machines. The reduction of ***c*1DC**$^{6+}$ necessarily involves a 'tightening' of the ultramacrocycle constituting its self-complexation, since the $V^{2+}$ unit is located much closer to $BB^{4+}$ than the DNP unit. The same can be said of the ultramacrocycle constituting ***c*2DC**$^{12+}$ except that, as a dimer with two end points, the reductive actuation of ***c*2DC**$^{12+}$ also results in net extension/contraction in molecular length. The [*a*2]daisy chain is essentially a [2]rotaxane in which the ring and dumbbell components are identical in their constitutions. Although no meaningful change in molecular dimensions accompanies this switching process, a net expansion and contraction of larger [*an*]daisy chain assemblies could in principle be realized.

## ■ CONCLUSIONS

We have reported the synthesis of blue box ($BB^{4+}$) daisy chains with 1,5-dioxynaphthalene (DNP) and viologen ($V^{2+}$) recognition units. Although these compounds can be switched electrochemically, they do not exhibit bistability in the ground state on account of electrostatic repulsion between the $BB^{4+}$ and $V^{2+}$ units. Instead, the rings encircle a DNP recognition unit exclusively in the ground state, but can adopt multiple co-conformations with respect to the stereochemistry of the $DNP\subset BB^{4+}$ donor−acceptor 'subcomplexes' they host. We here found, by $^1$H NMR spectroscopy, that the distribution of these co-conformational isomers and the activation barriers to their exchange processes depend on the architecture of the daisy chain, where the distributions are more biased and the energy barriers are greater in the smaller cyclic ([*c*1] and [*c*2]) daisy chains on account of steric constraints. Under sufficiently reducing conditions, the generation of bipyridinium radical cations causes the rings to move from the DNP units to the viologen units in favor of spin-paired $V^{\bullet+}\subset BB^{2(\bullet+)}$ subcomplexes, a phenomenon which has been observed by cyclic voltammetry and spectroelectrochemistry. Thus, we have (i) characterized six daisy chain architectures ([*c*1], [*c*2], [*c*3], [*a*1], [*a*2], [*a*3]) of which all but [*c*2] are represented by few to no examples in the literature, which are (ii) isolated from a single one-pot reaction, and (iii) utilize redox chemistry for switching to (iv) express unique modes of mechanical motion (e.g., constriction/dilation, expansion/contraction) in an all but quantitative manner. The high switching fidelity and unconventional mechanical motions generated by this redox-activated switching process in the cyclic daisy chains are particularly interesting in the context of designing molecular machines. We


dx.doi.org/10.1021/ja500675y | J. Am. Chem. Soc. 2014, 136, 4714−4723

are currently pursuing ways to orchestrate the concerted actuation of these molecular mechanical switches in a manner that will scale their potential to do workup to a macroscopic size regime.

## ■ ASSOCIATED CONTENT

### Supporting Information

Detailed synthetic procedures and characterization data (NMR and HRMS) for all compounds, spectroscopic (NMR and UV/vis) and electrochemical (CV) characterization of the daisy chain rotaxanes. This material is available free of charge via the Internet at http://pubs.acs.org.

## ■ AUTHOR INFORMATION


### Corresponding Authors

stoddart@northwestern.edu
s-stupp@northwestern.edu


### Notes

The authors declare no competing financial interest.

## ■ ACKNOWLEDGMENTS

This research was supported by the Non-Equilibrium Energy Research Center (NERC), an Energy Frontiers Research Center (EFRC) funded by the U.S. Department of Energy, Office of Science, Office of Basic Energy Sciences under Award Number DE-SC0000989. This research is part (Project 34-949) of the Joint Center of Excellence in Integrated Nano-Systems (JCIN) at King Abdul-Aziz City for Science and Technology (KACST) and Northwestern University (NU). The authors would like to thank both KACST and NU for their continued support of this research. C.J.B. acknowledges support from the National Science Foundation Graduate Research Fellowship Program.

## ■ REFERENCES


(1) (a) Schill, G. *Catenanes, Rotaxanes, and Knots*; Academic Press: New York, 1971. (b) Dietrich-Buchecker, C. O.; Sauvage, J.-P. *Chem. Rev.* **1987**, *87*, 795−810. (c) Amabilino, D. B.; Stoddart, J. F. *Chem. Rev.* **1995**, *95*, 2725−2829. (d) Sauvage, J.-P., Dietrich-Buchecker, C., Eds. *Catenanes, Rotaxanes, and Knots*; Wiley-VCH: Weinheim, 1999. (e) Stoddart, J. F. *Chem. Soc. Rev.* **2009**, *38*, 1802−1820.

(2) (a) Sauvage, J.-P. *Acc. Chem. Res.* **1998**, *31*, 611−619. (b) Balzani, V.; Gómez-López, M.; Stoddart, J. F. *Acc. Chem. Res.* **1998**, *31*, 405−414. (c) Balzani, V.; Credi, A.; Raymo, F. M.; Stoddart, J. F. *Angew. Chem., Int. Ed.* **2000**, *39*, 3348−3391. (d) Schalley, C.; Beizai, K.; Vögtle, F. *Acc. Chem. Res.* **2001**, *34*, 465−476. (e) Harada, A. *Acc. Chem. Res.* **2001**, *34*, 456−464. (f) Balzani, V.; Credi, A.; Ferrer, B.; Silvi, S.; Venturi, M. *Top. Curr. Chem.* **2005**, *262*, 1−27. (g) Kay, E. R.; Leigh, D. A.; Zerbetto, F. *Angew. Chem., Int. Ed.* **2007**, *46*, 72−191. (h) Balzani, V.; Credi, A.; Venturi, M. *Molecular Devices and Machines: Concepts and Perspectives for the Nanoworld*; Wiley-VCH: Weinheim, 2008. (i) Coskun, A.; Banaszak, M.; Astumian, R. D.; Stoddart, J. F.; Grzybowski, B. A. *Chem. Soc. Rev.* **2012**, *41*, 19−30.

(3) (a) Leigh, D. A.; Wong, J. K. Y.; Dehez, F.; Zerbetto, F. *Nature* **2003**, *424*, 174−179. (b) Badjić, J. D.; Balzani, V.; Credi, A.; Silvi, S.; Stoddart, J. F. *Science* **2004**, *303*, 1845−1849. (c) Liu, Y.; Flood, A. H.; Bonvallet, P. A.; Vignon, S. A.; Northrop, B. H.; Tseng, H.-R.; Jeppesen, J. O.; Huang, T. J.; Brough, B.; Baller, M.; Magonov, S.; Solares, S. D.; Goddard, W. A., III; Ho, C.-M.; Stoddart, J. F. *J. Am. Chem. Soc.* **2005**, *127*, 9745−9759. (d) Chuang, C.-J.; Li, W.-S.; Lai, C.-C.; Liu, Y.-H.; Peng, S.-M.; Chao, I.; Chiu, S.-H. *Org. Lett.* **2009**, *11*, 385−388. (e) Barin, G.; Coskun, A.; Friedman, D. C.; Olson, M. A.; Colvin, M. T.; Carmielli, R.; Dey, S. K.; Bozdemir, O. A.; Wasielewski, M. R.; Stoddart, J. F. *Chem.—Eur. J.* **2011**, *17*, 213−222. (f) Joosten, A.; Trolez, Y.; Collin, J.-P.; Heitz, V.; Sauvage, J.-P. *J. Am. Chem. Soc.* **2012**, *134*, 1802−1809.

(4) (a) Ashton, P. R.; Baxter, I.; Cantrill, S. J.; Fyfe, M. C. T.; Glink, P. T.; Stoddart, J. F.; White, A. J. P.; Williams, D. J. *Angew. Chem., Int. Ed.* **1998**, *37*, 1294−1297. (b) Rotzler, J.; Mayor, M. *Chem. Soc. Rev.* **2012**, *42*, 44−62.

(5) (a) Ashton, P. R.; Parsons, I. W.; Raymo, F. M.; Stoddart, J. F.; White, A. J. P.; Williams, D. J.; Wolf, R. *Angew. Chem., Int. Ed.* **1998**, *37*, 1913−1916. (b) Cantrill, S. J.; Youn, G. J.; Stoddart, J. F.; Williams, D. J. *J. Org. Chem.* **2001**, *66*, 6857−6872. (c) Fujimoto, T.; Nakamura, A.; Inoue, Y.; Sakata, Y.; Kaneda, T. *Tetrahedron Lett.* **2001**, *42*, 7987−7989. (d) Amirsakis, D. G.; Elizarov, A. M.; Garcia-Garibay, M. A.; Glink, P. T.; Stoddart, J. F.; White, A. J. P.; Williams, D. J. *Angew. Chem., Int. Ed.* **2003**, *42*, 1126−1132. (e) Wang, F.; Han, C.; He, C.; Zhou, Q.; Zhang, J.; Wang, C.; Li, N.; Huang, F. *J. Am. Chem. Soc.* **2008**, *130*, 11254−11255. (f) Zhang, Z.; Luo, Y.; Chen, J.; Dong, S.; Yu, Y.; Ma, Z.; Huang, F. *Angew. Chem., Int. Ed.* **2011**, *50*, 1397−1401. (g) Voignier, J.; Frey, J.; Kraus, T.; Budesinsky, M.; Cvacka, J.; Heitz, V.; Sauvage, J.-P. *Chem.—Eur. J.* **2011**, *17*, 5404−5414. (h) Zheng, B.; Wang, F.; Dong, S.; Huang, F. *Chem. Soc. Rev.* **2012**, *41*, 1621−1636. (i) Cao, L.; Isaacs, L. *Org. Lett.* **2012**, *14*, 3072−3075. (j) Yan, X.; Xu, D.; Chi, X.; Chen, J.; Dong, S.; Ding, X.; Yu, Y.; Huang, F. *Adv. Mater.* **2012**, *24*, 362−369.

(6) (a) Miyauchi, M.; Harada, A. *Chem. Lett.* **2005**, *34*, 104−105. (b) Miyauchi, M.; Hoshino, T.; Yamaguchi, H.; Kamitori, S.; Harada, A. *J. Am. Chem. Soc.* **2005**, *127*, 2034−2035. (c) Yamauchi, K.; Takashima, Y.; Hashidzume, A.; Yamaguchi, H.; Harada, A. *J. Am. Chem. Soc.* **2008**, *130*, 5024−5025. (d) Gibson, H. W.; Yamaguchi, N.; Niu, Z.; Jones, J. W.; Slebodnick, C.; Rheingold, A. L.; Zakharov, L. N. *J. Polym. Sci., Polym. Chem.* **2010**, *48*, 975−985. (e) Wang, F.; Zhang, J.; Ding, X.; Dong, S.; Liu, M.; Zheng, B.; Li, S.; Wu, L.; Yu, Y.; Gibson, H. W.; Huang, F. *Angew. Chem., Int. Ed.* **2010**, *49*, 1090−1094. (f) Dong, S.; Luo, Y.; Yan, X.; Zheng, B.; Ding, X.; Yu, Y.; Ma, Z.; Zhao, Q.; Huang, F. *Angew. Chem., Int. Ed.* **2011**, *50*, 1905−1909. (g) Strutt, N. L.; Zhang, H.; Giesener, M. A.; Lei, J.; Stoddart, J. F. *Chem. Commun.* **2012**, *48*, 1647−1649. (h) Wang, X.; Han, K.; Li, J.; Jia, X.; Li, C. *Polym. Chem.* **2013**, *4*, 3998−4003. (i) Rotzler, J.; Drayss, S.; Hampe, O.; Häussinger, D.; Mayor, M. *Chem.—Eur. J.* **2013**, *19*, 2089−2101.

(7) (a) Sasabe, H.; Inomoto, N.; Kihara, N.; Suzuki, Y.; Ogawa, A.; Takata, T. *J. Polym. Sci., Polym. Chem.* **2007**, *45*, 4154−4160. (b) Miyawaki, A.; Miyauchi, M.; Takashima, Y.; Yamaguchi, H.; Harada, A. *Chem. Commun.* **2008**, 456−458. (c) Zhang, M.; Li, S.; Dong, S.; Chen, J.; Zheng, B.; Huang, F. *Macromolecules* **2011**, *44*, 9629−9634.

(8) (a) Chiu, S.-H.; Rowan, S. J.; Cantrill, S. J.; Stoddart, J. F.; White, A. J. P.; Williams, D. J. *Chem. Commun.* **2002**, 2948−2949. (b) Guidry, E. N.; Li, J.; Stoddart, J. F.; Grubbs, R. H. *J. Am. Chem. Soc.* **2007**, *129*, 8944−8945. (c) Ueng, S.-H.; Hsueh, S.-Y.; Lai, C.-C.; Liu, Y.-H.; Peng, S.-M.; Chiu, S.-H. *Chem. Commun.* **2008**, 817−819. (d) Evans, N. H.; Beer, P. D. *Chem.—Eur. J.* **2011**, *17*, 10542−10546. (e) Bozdemir, O. A.; Barin, G.; Belowich, M. E.; Basuray, A. N.; Beuerle, F.; Stoddart, J. F. *Chem. Commun.* **2012**, *48*, 10401−10403. (f) Bruns, C. J.; Li, J.; Frasconi, M.; Schneebeli, S. T.; Iehl, J.; Jacquot de Rouville, H.-P.; Stupp, S. I.; Voth, G. A.; Stoddart, J. F. *Angew. Chem., Int. Ed.* **2014**, *53*, 1953−1958.

(9) Hoshino, T.; Miyauchi, M.; Kawaguchi, Y.; Yamaguchi, H.; Harada, A. *J. Am. Chem. Soc.* **2000**, *122*, 9876−9877.

(10) (a) Jiménez, M. C.; Dietrich-Buchecker, C.; Sauvage, J.-P. *Angew. Chem., Int. Ed.* **2000**, *39*, 3284−3287. (b) Collin, J.-P.; Dietrich-Buchecker, C.; Gaviña, P.; Jimenez-Molero, M. C.; Sauvage, J.-P. *Acc. Chem. Res.* **2001**, *34*, 477−487. (c) Jimenez-Molero, M. C.; Dietrich-Buchecker, C.; Sauvage, J.-P. *Chem. Commun.* **2003**, 1613−1616.

(11) (a) Dawson, R. E.; Lincoln, S. F.; Easton, C. J. *Chem. Commun.* **2008**, 3980−3982. (b) Li, S.; Taura, D.; Hashidzume, A.; Harada, A. *Chem.—Asian J.* **2010**, *5*, 2281−2289.

(12) (a) Wu, J.; Leung, K. C.-F.; Benítez, D.; Han, J.-Y.; Cantrill, S. J.; Fang, L.; Stoddart, J. F. *Angew. Chem., Int. Ed.* **2008**, *47*, 7470−7474. (b) Coutrot, F.; Romuald, C.; Busseron, E. *Org. Lett.* **2008**, *10*, 3741−

3744. (c) Romuald, C.; Busseron, E.; Coutrot, F. *J. Org. Chem.* **2010**, *75*, 6516−6531.
(13) (a) Romuald, C.; Ardá, A.; Clavel, C.; Jiménez-Barbero, J.; Coutrot, F. *Chem. Sci.* **2012**, *3*, 1851−1857. (b) Romuald, C.; Cazals, G.; Enjalbal, C.; Coutrot, F. *Org. Lett.* **2013**, *15*, 184−187.
(14) (a) Clark, P. G.; Day, M. W.; Grubbs, R. H. *J. Am. Chem. Soc.* **2009**, *131*, 13631−13633. (b) Fang, L.; Hmadeh, M.; Wu, J.; Olson, M. A.; Spruell, J. M.; Trabolsi, A.; Yang, Y.-W.; Elhabiri, M.; Albrecht-Gary, A.-M.; Stoddart, J. F. *J. Am. Chem. Soc.* **2009**, *131*, 7126−7134. (c) Hmadeh, M.; Fang, L.; Trabolsi, A.; Elhabiri, M.; Albrecht-Gary, A.-M.; Stoddart, J. F. *J. Mater. Chem.* **2010**, *20*, 3422−3430. (d) Du, G.; Moulin, E.; Jouault, N.; Buhler, E.; Giuseppone, N. *Angew. Chem., Int. Ed.* **2012**, *51*, 12504−12508.
(15) Bruns, C. J.; Stoddart, J. F. *Nature Nanotechnol.* **2012**, *8*, 9−10.
(16) (a) Odell, B.; Reddington, M. V.; Slawin, A. M. Z.; Spencer, N.; Stoddart, J. F.; Williams, D. J. *Angew. Chem., Int. Ed. Engl.* **1988**, *27*, 1547−1550. (b) Stoddart, J. F.; Colquhoun, H. M. *Tetrahedron* **2008**, *64*, 8231−8263. (c) Gong, H.-Y.; Rambo, B. M.; Karnas, E.; Lynch, V. M.; Sessler, J. L. *Nature Chem.* **2010**, *2*, 406−409. (d) Biedermann, F.; Vendruscolo, M.; Scherman, O. A.; De Simone, A.; Nau, W. M. *J. Am. Chem. Soc.* **2013**, *135*, 14879−14888.
(17) (a) Asakawa, M.; Ashton, P. R.; Menzer, S.; Raymo, F.; Stoddart, J. F.; White, A. J. P.; Williams, D. J. *Chem.—Eur. J.* **1996**, *2*, 877−893. (b) Barnes, J. C.; Juríček, M.; Strutt, N. L.; Frasconi, M.; Sampath, S.; Giesener, M. A.; McGrier, P. L.; Bruns, C. J.; Stern, C. L.; Sarjeant, A. A.; Stoddart, J. F. *J. Am. Chem. Soc.* **2013**, *135*, 183−192. (c) Juríček, M.; Barnes, J. C.; Dale, E. J.; Liu, W.-G.; Strutt, N. L.; Bruns, C. J.; Vermeulen, N. A.; Ghooray, K.; Sarjeant, A. A.; Stern, C. L.; Botros, Y. Y.; Goddard, W. A., III; Stoddart, J. F. *J. Am. Chem. Soc.* **2013**, *135*, 12736−12746. (d) Barnes, J. C.; Juríček, M.; Vermeulen, N. A.; Dale, E. J.; Stoddart, J. F. *J. Org. Chem.* **2013**, *78*, 11962−11969.
(18) (a) Olson, M. A.; Botros, Y. Y.; Stoddart, J. F. *Pure Appl. Chem.* **2010**, *82*, 1569−1574. (b) Vignon, S. A.; Stoddart, J. F. *Collect. Czech. Chem. Commun.* **2005**, *70*, 1493−1576.
(19) Fahrenbach, A. C.; Bruns, C. J.; Cao, D.; Stoddart, J. F. *Acc. Chem. Res.* **2012**, *45*, 1581−1592.
(20) Fahrenbach, A. C.; Bruns, C. J.; Li, H.; Trabolsi, A.; Coskun, A.; Stoddart, J. F. *Acc. Chem. Res.* **2014**, *47*, 482−493.
(21) Coskun, A.; Spruell, J. M.; Barin, G.; Dichtel, W. R.; Flood, A. H.; Botros, Y. Y.; Stoddart, J. F. *Chem. Soc. Rev.* **2012**, *41*, 4827−4859.
(22) Trabolsi, A.; Khashab, N.; Fahrenbach, A. C.; Friedman, D. C.; Colvin, M. T.; Cotí, K. K.; Benítez, D.; Tkatchouk, E.; Olsen, J.-C.; Belowich, M. E.; Carmielli, R.; Khatib, H. A.; Goddard, W. A., III; Wasielewski, M. R.; Stoddart, J. F. *Nature Chem.* **2010**, *2*, 42−49.
(23) (a) Fahrenbach, A. C.; Barnes, J. C.; Lanfranchi, D. A.; Li, H.; Coskun, A.; Gassensmith, J. J.; Liu, Z.; Benítez, D.; Trabolsi, A.; Goddard, W. A., III; Elhabiri, M.; Stoddart, J. F. *J. Am. Chem. Soc.* **2012**, *134*, 3061−3072. (b) Fahrenbach, A. C.; Sampath, S.; Late, D. J.; Barnes, J. C.; Kleinman, S. L.; Valley, N.; Hartlieb, K. J.; Liu, Z.; Dravid, V. P.; Schatz, G. C.; Van Duyne, R. P.; Stoddart, J. F. *ACS Nano* **2012**, *6*, 9964−9971. (c) Barin, G.; Frasconi, M.; Dyar, S. M.; Iehl, J.; Buyukcakir, O.; Sarjeant, A. A.; Carmieli, R.; Coskun, A.; Wasielewski, M. R.; Stoddart, J. F. *J. Am. Chem. Soc.* **2013**, *135*, 2466−2469.
(24) (a) Li, H.; Fahrenbach, A. C.; Dey, S. K.; Basu, S.; Trabolsi, A.; Zhu, Z.; Botros, Y. Y.; Stoddart, J. F. *Angew. Chem., Int. Ed.* **2010**, *49*, 8260−8265. (b) Barnes, J. C.; Fahrenbach, A. C.; Cao, D.; Dyar, S. M.; Frasconi, M.; Giesener, M. A.; Benítez, D.; Tkatchouk, E.; Chernyashevskyy, O.; Shin, W. H.; Li, H.; Sampath, S.; Stern, C. L.; Sarjeant, A. A.; Hartlieb, K. J.; Liu, Z.; Carmieli, R.; Botros, Y. Y.; Choi, J. W.; Slawin, A. M. Z.; Ketterson, J. B.; Wasielewski, M. R.; Goddard, W. A., III; Stoddart, J. F. *Science* **2013**, *339*, 429−433. (c) Li, H.; Zhu, Z.; Fahrenbach, A. C.; Savoie, B. M.; Ke, C.; Barnes, J. C.; Lei, J.; Zhao, Y.-L.; Lilley, L. M.; Marks, T. J.; Ratner, M. A.; Stoddart, J. F. *J. Am. Chem. Soc.* **2013**, *135*, 456−467.
(25) (a) Li, H.; Fahrenbach, A. C.; Coskun, A.; Zhu, Z.; Barin, G.; Zhao, Y.-L.; Botros, Y. Y.; Sauvage, J.-P.; Stoddart, J. F. *Angew. Chem., Int. Ed.* **2011**, *50*, 6782−6788. (b) Barnes, J. C.; Fahrenbach, A. C.; Dyar, S. M.; Frasconi, M.; Giesener, M. A.; Zhu, Z.; Liu, Z.; Hartlieb, K. J.; Carmieli, R.; Wasielewski, M. R.; Stoddart, J. F. *Proc. Natl. Acad. Sci. U.S.A.* **2012**, *109*, 11546−11551. (c) Zhu, Z.; Fahrenbach, A. C.; Li, H.; Barnes, J. C.; Liu, Z.; Dyar, S. M.; Zhang, H.; Lei, J.; Carmieli, R.; Sarjeant, A. A.; Stern, C. L.; Wasielewski, M. R.; Stoddart, J. F. *J. Am. Chem. Soc.* **2012**, *134*, 11709−11720. (d) Fahrenbach, A. C.; Zhu, Z.; Cao, D.; Liu, W.-G.; Li, H.; Dey, S. K.; Basu, S.; Trabolsi, A.; Botros, Y. Y.; Goddard, W. A., III; Stoddart, J. F. *J. Am. Chem. Soc.* **2012**, *134*, 16275−16288.
(26) The term 'ouroboros', from the Greek roots ourá (tail) and boros (to eat), refers to the ancient alchemical symbol of a tail-eating serpent, which also allegedly appeared to Kekule in the dream that led him to the correct structure of benzene. [*c*1]Daisy chains have been dubbed 'ouroboros' because their self-complexing character resembles the self-devouring serpent of the same name. See: (a) Nygaard, S.; Liu, Y.; Stein, P. C.; Flood, A. H.; Jeppesen, J. O. *Adv. Funct. Mater.* **2007**, *17*, 751−762. (b) Nielsen, K. A.; Bähring, S.; Jeppesen, J. O. *Chem.—Eur. J.* **2011**, *17*, 11001−11007.
(27) (a) Ashton, P. R.; Campbell, P. J.; Chrystal, E. J. T.; Glink, P. T.; Menzer, S.; Philp, D.; Spencer, N.; Stoddart, J. F.; Tasker, P. A.; Williams, D. J. *Angew. Chem., Int. Ed. Engl.* **1995**, *34*, 1865−1869. (b) Kolchinski, A. G.; Busch, D. H.; Alcock, N. W. *J. Chem. Soc., Chem. Commun.* **1995**, 1289−1291.
(28) (a) Olson, M. A.; Braunschweig, A. B.; Ikeda, T.; Fang, L.; Trabolsi, A.; Slawin, A. M. Z.; Khan, S. I.; Stoddart, J. F. *Org. Biomol. Chem.* **2009**, *7*, 4391−4405. (b) Boyle, M. M.; Gassensmith, J. J.; Whalley, A. C.; Forgan, R. S.; Smaldone, R. A.; Hartlieb, K. J.; Blackburn, A. K.; Sauvage, J.-P.; Stoddart, J. F. *Chem.—Eur. J.* **2012**, *18*, 10312−10323.
(29) (a) Liu, Y.; Flood, A. H.; Stoddart, J. F. *J. Am. Chem. Soc.* **2004**, *126*, 9150−9151. (b) Liu, Y.; Flood, A. H.; Moskowitz, R. M.; Stoddart, J. F. *Chem.—Eur. J.* **2005**, *11*, 369−385.
(30) Liu, Y.; Saha, S.; Vignon, S. A.; Flood, A. H.; Stoddart, J. F. *Synthesis* **2005**, 3437−3445.
(31) (a) Liu, Y.; Vignon, S. A.; Zhang, X.; Bonvallet, P. A.; Khan, S. I.; Houk, K. N.; Stoddart, J. F. *J. Org. Chem.* **2005**, *70*, 9334−9344. (b) Liu, Y.; Vignon, S. A.; Zhang, X.; Houk, K. N.; Stoddart, J. F. *Chem. Commun.* **2005**, 3927−3929. (c) Liu, Y.; Bonvallet, P. A.; Vignon, S. A.; Khan, S. I.; Stoddart, J. F. *Angew. Chem., Int. Ed.* **2005**, *44*, 3050−3055. (d) Zhao, Y.-L.; Trabolsi, A.; Stoddart, J. F. *Chem. Commun.* **2009**, 4844−4846.
(32) Cao, D.; Wang, C.; Giesener, M. A.; Liu, Z.; Stoddart, J. F. *Chem. Commun.* **2012**, *48*, 6791−6793.
(33) Hänni, K. D.; Leigh, D. A. *Chem. Soc. Rev.* **2010**, *39*, 1240−1251.
(34) Zhu, Z.; Bruns, C. J.; Li, H.; Lei, J.; Ke, C.; Liu, Z.; Shafaie, S.; Colquhoun, H. M.; Stoddart, J. F. *Chem. Sci.* **2013**, *4*, 1470−1483.
(35) Since a noncovalent assembly comprising two or more distinct chemical entitites is often described as a 'complex', we use the term 'subcomplex' to describe a local noncovalent associative interaction within a larger supramolecular assembly or mechanically interlocked molecule.
(36) Note that the rotation of the Ph and $BIPY^{2+}$ rings are also dynamic processes which can be investigated by $^1H$ NMR spectroscopy, but they are not responsible for any isomerization on account of their symmetrical constitutions.
(37) (a) Kosower, E. M.; Hajdu, J. *J. Am. Chem. Soc.* **1971**, *93*, 2534−2535. (b) Geuder, W.; Hünig, S.; Suchy, A. *Tetrahedron* **1986**, *42*, 1665−1677.